

# Upgrading the seismic capacity of RC buildings using chevron buckling restrained braces

Fozeya O. Algennay

E-mail: [fozeya.algenai@su.edu.ly](mailto:fozeya.algenai@su.edu.ly)

Structural engineering Department, Faculty of engineering, Sirt University, Libya.

## Abstract

Many RC buildings do not meet the lateral strength requirements of current seismic codes and are vulnerable to significant damage or collapse in the event of future earthquakes. Several systems are available for seismic strengthening of RC buildings such as enlargement of the structural members and adding new structural shear walls.

In the past few decades, buckling-restrained braces have become popular as a lateral force resisting system because of their capability of improving the strength, the stiffness and the energy absorbing capacity of structures. This study evaluates the seismic upgrading of a 6-story RC building using chevron buckling restrained braces. Seismic evaluation in this study has been carried out by static pushover analysis and time history earthquake analysis. Ten ground motions with different PGA levels are used in the analysis. The mean plus one standard deviation values of the roof-drift ratio, the maximum story drift ratio, the brace ductility factors and the member strain responses are used as the basis for the seismic performance evaluations. The results obtained in this study indicate that strengthening of RC buildings with buckling restrained braces is an efficient technique as it significantly increases the PGA capacity of the RC buildings. The results also indicate the increase in the PGA capacity of the RC building with the increase in the amount of the braces.

The use of BRBs in one bay in each of the perimeter frames of the RC building results in a significant improvement to the base shear capacity of the RC building. In the current study, an increase in the base shear capacity up to 150% from the base shear capacity of the original RC building has been achieved by the BRBs.

**Keywords:** : roof drift, story drift, strain, buckling restrained brace, earthquake, pushover analysis, dynamic analysis, strength, seismostruct.

## 1. Introduction

Many existing buildings do not meet the lateral strength requirements of current seismic codes. This lateral load resistance inadequacy may arise due various reasons which include; (a) the design of the building according earlier versions of code provisions using gravity loads only (b)

subsequent updating of seismic codes and the intensity of seismic hazard in order to minimize the level of damage and repair costs after an earthquake, (c) modifications in existing buildings, (d) change in the building use (e) strength deterioration due to aging or previous earthquakes. These buildings are vulnerable to significant damage or collapse in the event of future earthquakes.

Different retrofitting techniques can be used to improve the seismic capacity of existing RC buildings. These techniques include jacketing and inserting new elements in the existing RC building such as shear walls or conventional steel bracings.

Jacketing of the RC members can significantly improve the strength, the stiffness and the ductility of those members. The beam-column joints as well as the columns are regarded as the most critical structural members to be jacketed. The jacketing technique requires working on all the building elements and this requires evacuating the whole building. In addition, the jacketing technique is labor-intensive due to the associated heavy demolition and construction works.

Inserting shear wall elements in the existing RC building improves the building lateral strength and stiffness. In addition, it has the advantage of concentrating the construction work in few places of the building. However there are several disadvantages to this approach which include the need for new foundations or strengthening of the existing ones.

Conventional steel bracing have been used in seismic strengthening of RC buildings in areas of high seismicity. They can be more rapidly installed than other strengthening techniques and they do not add much weight to the structure. The bracing system can be attached to the perimeter frames of the building and consequently, disruptions are minimized during construction. The hysteretic behavior of conventional steel braces is un-symmetric in tension and compression. The yielding of the braces in tension under lateral loading provides a ductile plastic mechanism with a good source of energy dissipation. On the other hand, brace buckling in compression provides a poor source of energy dissipation because of the post-buckling behavior of the braces which is characterized by deterioration of strength and stiffness.

Masri and Goel [1], Bush et al. [2], Maheri and Sahebi[3], and Liu et al.[4] studied experimentally the effectiveness of using steel braces to retrofit existing RC frames. They reported that such a method allows upgrading the seismic capacity of existing structures. Their experimental results highlight the effectiveness of the steel brace strengthening technique in improving the global performance of RC structures in terms of strength, ductility and energy dissipation. Comparative studies of seismic strengthening of RC buildings by steel braces and other systems such as column jacketing and RC infill walls have been conducted by Alashkar[5], Farghaly and Abdallah[6], and Ibrahim [7]. The results of these studies showed that better improving can be attained by using concentric steel braces than other strengthening techniques.

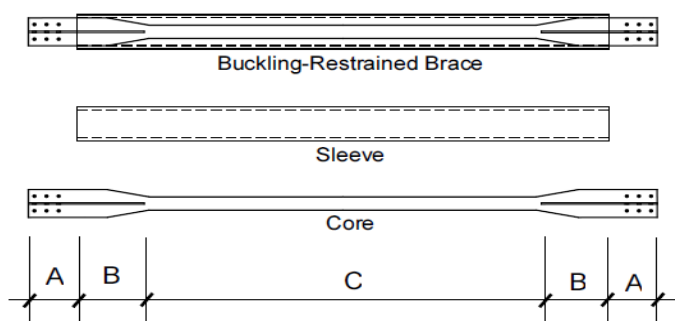
Hosseini et al [8], studied the use of eccentric steel braces for the retrofit of existing RC frame buildings. Vertical steel links attached at the middle of the RC beams and inverted-V concentric steel braces were utilized in their study. The nonlinear static analysis results indicate that the

inverted Y steel bracing system is an alternative way to construct ductile structures with greater lateral stiffness.

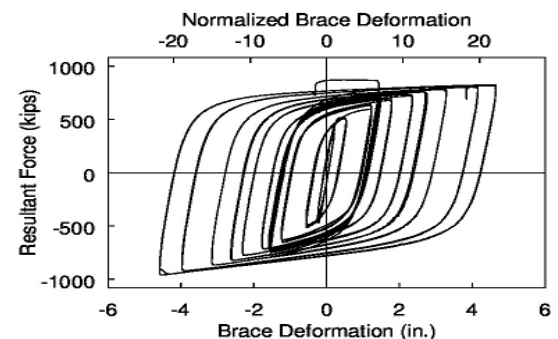
Buckling-Restrained Braces (BRBs) have become one of the most efficient earthquake-resistant structural systems and have been actively applied to seismic design and retrofit of building structures in regions with high seismicity. BRBs do not exhibit any unfavorable behavior characteristics of concentric braces and they allow using less steel and simpler joints in comparison with other construction methods.

Figure.1 [9] shows the BRB components which consists of a steel core and external jacket. The steel core is subjected to inelastic deformations under the effect of lateral loading and the external jacket serve in restraining buckling of the steel core element. The steel core is divided into three segments; the yielding zone, transition zone and the connection zone. The yielding zone has a reduced cross section and is fully restrained to insure the occurrence of tensile and compressive yielding. The transition zones are the segments of the brace directly on either side of the yielding zone. These segments have larger cross sectional area than the yielding zone but are similarly restrained. The connection zone is the portion of the brace that extends beyond the restraining components and is used to connect the brace to other structural elements of the frame.

The steel core can be a rod, a single plate, or a built-up section and the external jacket can be made of steel tube filled with mortar. A gap between the steel core and the mortar must be set to ensure that the axial stresses are resisted by the steel core only and not by the jacket, the BRBs are expected to yield in both tension and compression with a stable hysteretic behaviour because of the lateral restraint provided by the external jacket (Newell et al. 2006). Typical BRB patterns are shown in figure. 2[10]



**Figure1 :** Schematic diagram of the BRB components [10]



**Figure 2:** Axial force versus axial displacement of BRB [10]

Analytical and experimental studies carried out on structures with BRBs Clark et al. [11], conducted a study that compared the seismic performance of a special moment resisting frame and a BRB frame. The total weight of steel in the BRB frame was reduced significantly by 50% compared to the moment resisting frame.

BRB possesses large ductility capacity and the cumulative inelastic deformation in BRBs under cyclic loading can exceed 300 times the initial yield deformation before failure, Sabelli et al., [9], Large-scale tests were conducted by Fahnestock et al. [12], These experimental evaluations were

conducted to demonstrate the performance of the system when subjected to multiple earthquake simulations and investigated the poor performance at story drifts between 0.02 and 0.025 radians.

Sarno and Elnashai [13], conducted a study that assessed the seismic performance of steel moment resisting frames (MRF) retrofitted with different bracing systems. The original MRF was designed with a lateral stiffness that didn't comply with drift limitations in high seismic region. The bracing systems were special concentrically braced frames, mega-braces and BRBF. Deulkar et al. [14], investigated the effect of BRB design parameter such as overall length and cross sectional area of yielding core proposed a new brace configuration for BRB.

Examples of new BRB configurations include the hybrid buckling restrained braced frames [15], which help to prevent excessive damage on the system under frequent low-to-mid intensity ground motions, and the self-centering BRB [16], incorporating a shape memory alloy which helps in self-centering to reduce residual deformations under seismic loading.

The purpose of this study is to evaluate the seismic upgrading of an existing 6-story RC frame using buckling restrained braces. The existing RC building is assumed to be designed based on the current provisions of the Egyptian code [17, 18]. the chevron buckling restrained brace patterns are assessed in this study. Three target strength levels of 50%, 100% and 150% from the original base shear capacity of the RC building are considered in the design of the braces. Seismic evaluation in this study has been carried out by static pushover analysis and time history earthquake analysis. Ten ground motions with different PGA levels are used in the analysis. The mean plus one standard deviation values of the roof-drift ratio, the maximum story drift ratio, brace axial ductility demand and the maximum element-strain responses are used as the basis for the seismic performance evaluations.

## **2. Prototype-Building and Computer Program**

---

The prototype building is a 6-story office building located in Cairo, Egypt. The building has a rectangular plan configuration as shown in figure (3). The plan of the building is 25 m long and 15 m wide. Seismic force resistance is provided by RC moment resisting frames in both directions. The elevation of the RC frames in the short direction is illustrated in figure (4). The first story of the building is 4 m height and the other stories are 3 m height. Concrete with a characteristic cubic strength (f<sub>cu</sub>) of 25 MPa is used together with reinforcing steel bars (36/52), with yield and ultimate strengths of 360 MPa and 520 MPa, respectively. Modulus of elasticity of steel is considered equal to 200 GPa.

For gravity loads, 2.5kPa and live load is assumed and 8.0kPa dead load is considered which includes the weights of 12cm RC slab, columns, beams, floor cover and the wall partitions. Lateral loads are determined according to the ECP-201 [17]. The seismic mass is considered equal to the dead load plus half of the live load. The building is assumed to be located on soil type 'C' and in seismic zone 3 with a design ground acceleration of 0.15g which is associated with 10% probability of exceedance in 50 years.

The applied loads are factored and combined according to the specification of ECP-203 [18] and the straining actions (moments, shears and axial forces) are obtained using the computer program SAP2000. The principle of weak beam strong column connection is applied in the design. The cross section and reinforcement details of the interior and exterior RC frames in the short direction are shown in tables 1 and 2.

**Table1:** Dimension of section and reinforcement details of columns

Column	Internal frame	External frame		
	Dimensions(mm)	reinforcement	Dimensions(mm)	reinforcement
Exterior	350×350	8Ø16	350×350	8Ø16
Interior	500×500	8Ø20	400×400	8Ø20

**Note:** the columns reinforcement is distributed symmetrical along the column sides

**Table2:** Reinforcement details of beams

Beam	Internal frame		External frame	
	Top reinforcement	Bottom reinforcement	Top reinforcement	Bottom reinforcement
B <sub>1</sub>	4Ø16	2Ø16	4Ø16	2Ø16
B <sub>2</sub>	3Ø16	2Ø16	4Ø16	2Ø16
B <sub>3</sub>	3Ø16	2Ø16	3Ø16	2Ø16

All beams have same size (250×500mm)

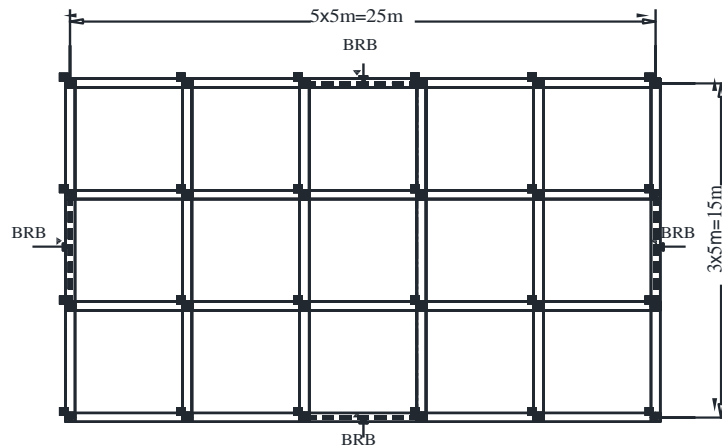


**Figure 3:** Typical floor plan of the prototype building.

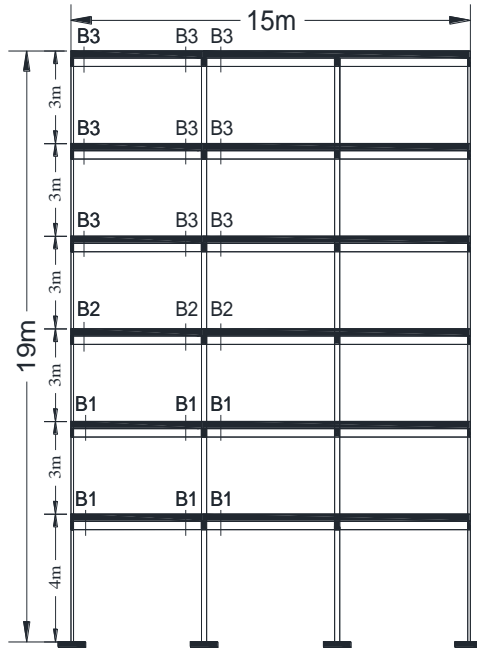


**Figure 4:** Typical frame elevation in the short direction

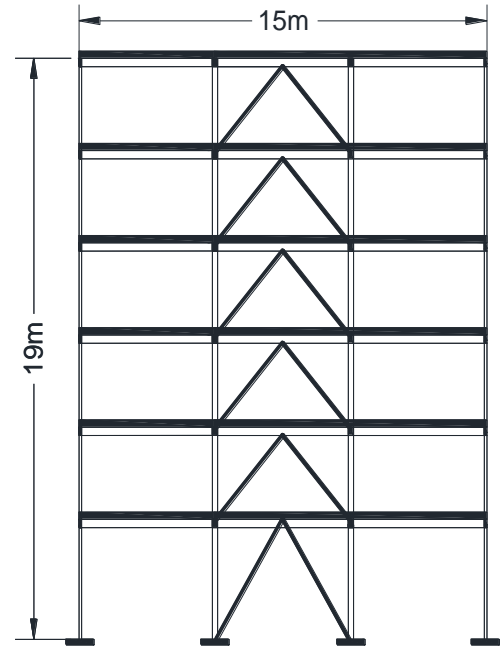
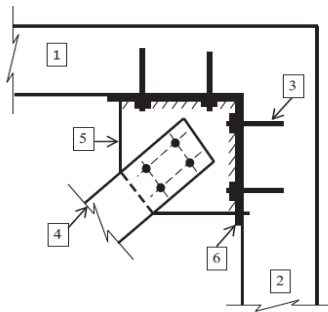


**Figure 5:** Chevron brace pattern

## 2.1BRB design

The BRBs are assumed to be attached to the perimeter frames of the RC building with buckling restrained brace patterns including the chevron braces are considered in this study and are shown in Figures(5). Only, the two perimeter braced frames in the short direction are designed and analyzed in the current study. The BRBs are designed to achieve three target strength levels of 50%, 100% and 150% from the original base shear capacity of the RC frame in the short direction. The designed BRB frames are denoted  $C_1$ ,  $C_2$  and  $C_3$  for the case of chevron brace configuration. Table3 .summarized the characteristics of the braced cases considered in the current study. The cross sections of the BRB cores are presented in table 4 and the BRB geometry is considered as demonstrated in Figure(1). The axial force in the BRB is equal to the story shear divided by cosine the brace inclination angle and the BRB yield strength is considered equal to 360 MPa. with considering the yielding zone length equals to half the total length and the cross sectional areas of the transition and the connection zones equal to five times the cross-sectional area of the yielding zone. The connection between the BRBs and the RC frame can be achieved by welding a gusset plates to steel plates that are anchored to the concrete frame as shown in Figure (6). Special care must be taken in designing the connection by calculating the forces acting on the anchors and the weld in order to avoid a premature failure of the connections.



1	RC beam	4	Steel brace
2	RC column	5	Gusset plate
3	Anchor bolt	6	Steel plate

**Figure 6:** Concept of beam -to- column connection

Braced case	Bracing strength* (%)	Configuration
C <sub>1</sub>	50	Chevron
C <sub>2</sub>	100	Chevron
C <sub>3</sub>	150	Chevron
Bracing strengths calculated as a percentage from the base shear capacity of the original RC frame.		

**Table 3:** Characteristics of the braced cases considered in this stud

Story Number	Area (cm <sup>2</sup> )		
	C <sub>1</sub>	C <sub>2</sub>	C <sub>3</sub>
1	12.11	24	30
2	9.5	18.8	25
3	8.4	16.8	22
4	7	13.9	19
5	5	10	15.3
6	2.7	5.5	8.28

**Table 4:** BRB-core cross sections of the of the design cases (cm<sup>2</sup>)

## 2.2 Jacketing of the braced-bay columns

Bracing of the perimeter frames imposes significant axial force demands on the columns and the foundations of the braced bay. Axial force demands on the braced-bay columns correspond to the ultimate capacity of the BRBs are presented in Table 5 along with the axial load capacity of the columns. The tensile capacity of the columns in tension is calculated by considering only the steel reinforcement tensile capacity. The results presented in table 5 indicate the need for cross section enlargement of the first three-story columns for the three braced cases S<sub>1</sub>, S<sub>2</sub> and S<sub>3</sub> as summarized in table 6. In addition cross section enlargement is also required for the top three-story columns for the braced case S<sub>3</sub> as shown in Table 6.

**Table 5:** Axial force demands and capacities of the braced-bay columns

Story number	Case	Axial force capacity (kN)		Axial force demands (kN)	
		Compression	Tension	Compression	Tension
1,2,3	C <sub>1</sub>	2006	786.76	203.23	203.23
	C <sub>2</sub>	2006	786.76	1634.3	1634.3
	C <sub>3</sub>	2006	786.76	2512	2512
4,5,6	C <sub>1</sub>	2006	786.76	199.72	199.72
	C <sub>2</sub>	2006	786.76	397.93	397.93
	C <sub>3</sub>	2006	786.76	779.87	779.87

**Table 6:** Dimensions and reinforcement details of the modified columns

Story number	Case	Dimensions of the modified column	Jacket reinforcement
1,2,3	C <sub>1</sub>	No modification	-
	C <sub>2</sub>	50×50	12Ø20
	C <sub>3</sub>	50×50	16Ø22
4,5,6	C <sub>1</sub>	No modification	-
	C <sub>2</sub>	No modification	-
	C <sub>3</sub>	No modification	-

### 3. Computer modeling

The six-story building is analytically modeled as a series of planar frames connected at each floor level by rigid diaphragms. Because of the building’s symmetry, only half of the building frames in the short direction are considered in the analytical model as shown in Figure (7). The building model includes one external braced frame and two internal unbraced frames and is assigned half of the building mass to simulate the actual behavior of the structure during the earthquake application.

The computer analysis has been carried out using the SeismoStruct computer program [19]. The SeismoStruct computer program is a finite element program that is capable of predicting the behavior of structures under static or dynamic loading, taking into account both geometric and material nonlinearities. Beams and columns are modeled using the force-based beam-column element that utilizes the fiber modeling approach to capture the spread of inelasticity along the member length. The member is subdivided into segments distributed along the member length, and

the cross section of each segment is subdivided into concrete and steel fibers. A uniaxial bilinear stress-strain model with kinematic strain hardening is assigned for the steel fibers. The concrete was modeled using a uniaxial nonlinear constant confinement concrete model that follows the constitutive relationship proposed by Mander et al. [20] and the cyclic rules proposed by Martinez-Rueda and Elnashai.[21]. The sectional response is obtained through the integration of the nonlinear uniaxial stress-strain response of the individual fibers forming the cross-section while the member response is obtained by integrating sectional responses along the member length.

The BRBs are modeled using a pin-ended element with uniform cross section and with a uniaxial bilinear stress-strain model that has a kinematic strain hardening. A modified modulus of elasticity and strain hardening parameter are calculated for the SeismoStruct element to account for the varying cross section of the BRBs.

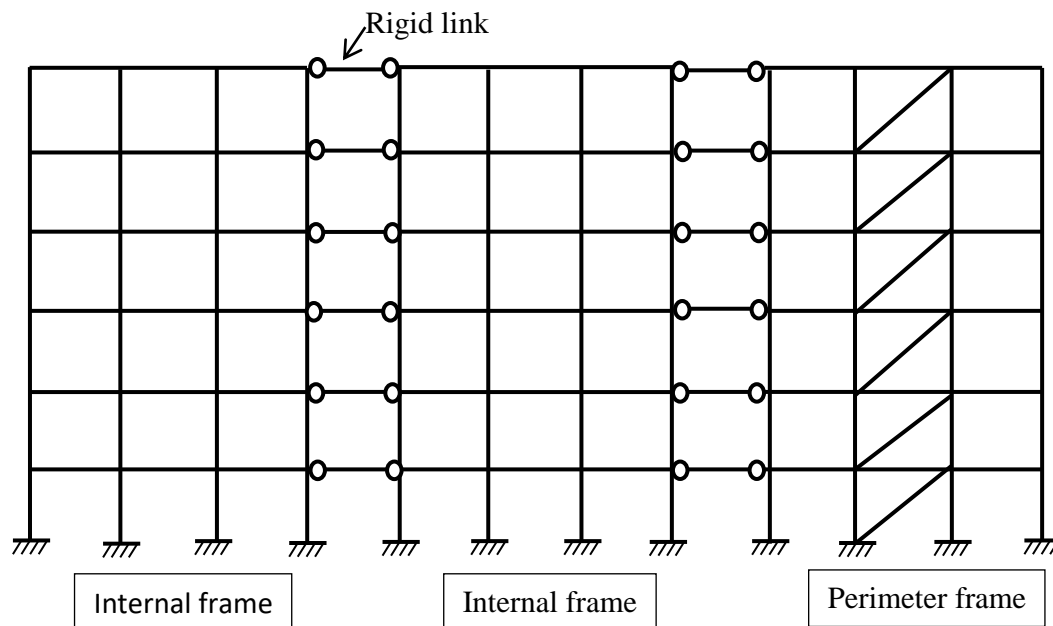


**Figure 7:** Planar representation of the RC building

#### 4. Pushover analysis of frames with single diagonal braces

Performance assessment of the designed frames is carried out using nonlinear static pushover analysis. The results of the pushover analysis obtained using the SeismoStruct computer program provide information on the base shear capacity as well as the distributions of the story displacements of the investigated frames. These data are important in evaluating the strength capacity and the overall ductility of the frames. Moreover, local behavior of the frame members from the pushover analysis is essential in determining the frame critical-elements. Pushover

analysis is performed until reaching 2% roof drift ratio using the lateral load distribution pattern specified in the Egyptian code. Gravity loads are applied on the frame during the pushover and is taken equal to the dead loads plus half of the live load.

Figure. (8) shows the relationships between the base-shear coefficient and the roof drift ratios of the original RC frame and the three braced cases  $C_1$ ,  $C_2$  and  $C_3$ . The base-shear coefficient is defined as the base shear divided by the building weight. The results shown in Figure (8) indicate that the ultimate strengths of the three braced cases  $C_1$ ,  $C_2$  and  $C_3$  are 142.8%, 187% and 220 % from the ultimate strength of the original RC frame. Moreover, the initial lateral stiffness of the three braced cases  $C_1$ ,  $C_2$  and  $C_3$  are 180%, 238% and 280 % from the initial lateral stiffness of the original RC frame.

Figure(9) shows the distributions of story drift ratios along the frame height of the original RC frame and the three braced cases  $C_1$ ,  $C_2$  and  $C_3$  at 2.0% roof drift ratio. The results shown in Figure(9) indicate a significant improvement in the distribution of story drifts with the increase in the amount of the braces. The maximum story drift ratios of the original RC frame and the three braced cases  $C_1$ ,  $C_2$  and  $C_3$  reached 4.1%, 4.2%, 5.25% and 5.1%, respectively.

The column strain factor of a specific story is calculated as the maximum strain in the steel reinforcement of the story columns divided by the steel yield strain ( $\epsilon_y = 0.0017$ ). Figure.9 shows the distribution of column strain factors along the frame height at 2% roof drift ratio. The results presented in Figure (10) indicate the increase in the column strain factors with the increase in the amount of steel braces. This behavior can be attributed to the axial force increase in the frame columns due to the existing of the BRBs. The maximum column strain factors occurred at the first and the second story columns and reached 2.5, 2.7, 3.64 and 5.8 for the original RC frame and the three braced cases  $C_1$ ,  $C_2$  and  $C_3$ , respectively. The beam strain factor of a specific story is also calculated as the maximum strain in the steel reinforcement of the story beams divided by the steel yield strain. Figure. 11 shows the distribution of beam strain factors along the frame height at 2% roof drift ratio. The beam strain factors reached 21.7, 24.7, 31.17 and 29 for the original RC frame and the three braced cases  $C_1$ ,  $C_2$  and  $C_3$ , respectively. The results presented in Figure(11) indicate that the maximum beam strain factors occurred in the first story beams in the original frame and the braced cases  $C_1$  and  $C_2$  and  $C_3$ . The results of Figure (11) indicate improvement in the distribution of beam strain factors along the frame stories with the increase in the amount of the braces.

The maximum BRB ductility demands are calculated as the maximum change in brace length divided by the brace yield displacement in tension. Figure (12) shows the distribution of the BRB ductility demands along the frame height due to the pushover loading.

The results illustrated in Figure (12) indicate that the BRB ductility demands reached 7.9, 7.5, and 0.7 for the braced cases C<sub>1</sub>, C<sub>2</sub> and C<sub>3</sub>, respectively. The reduction in the BRBs ductility demands of the braced case C<sub>3</sub> is attributed to area of the BRB bracing in this braced case.

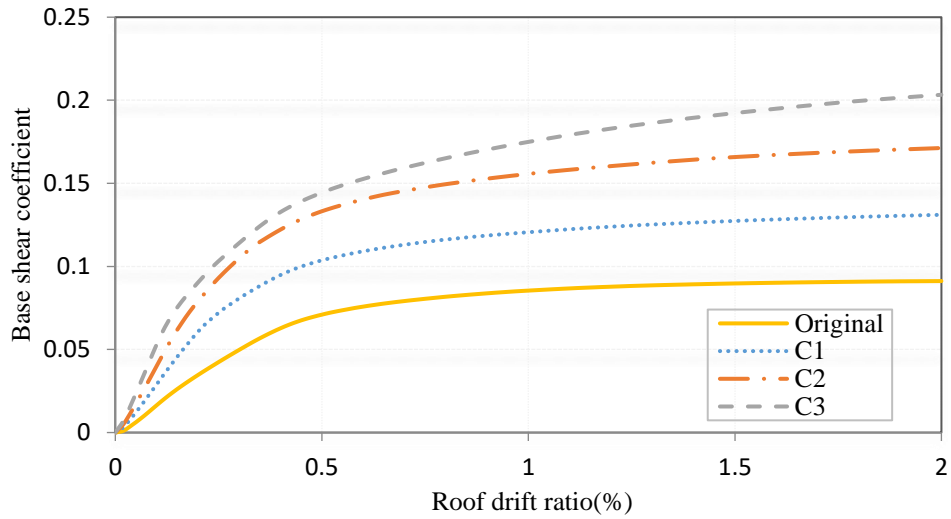


**Figure 8:** The relationships between base shear coefficient and roof drift ratio due to pushover analysis

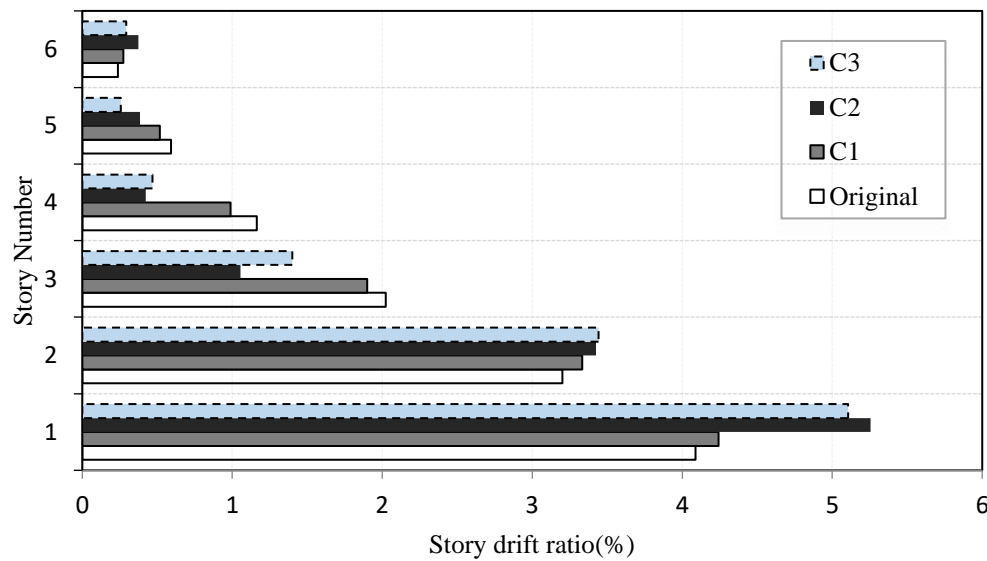


**Figure 9:** Distribution of story drift ratios at 2% Roof drift ratio due to pushover analysis

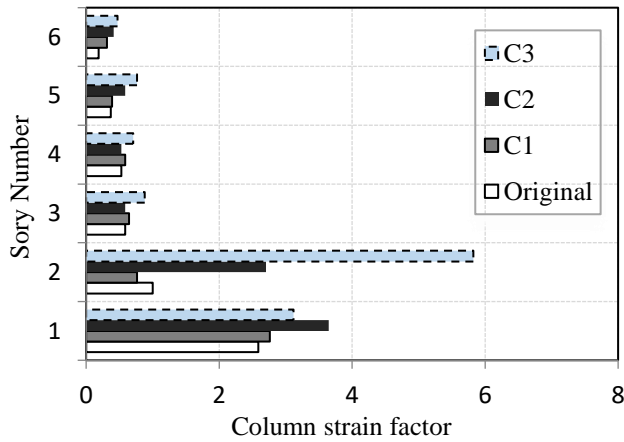


**Figure 10:** The distributions of column strain factors at 2% roof drift ratio due to pushover loading.

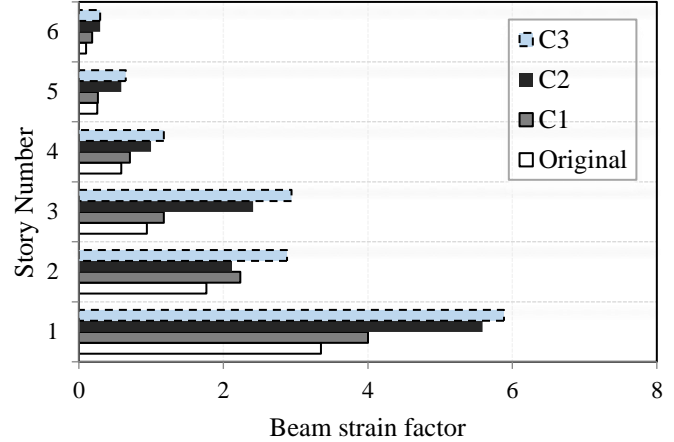


**Figure 11:** The distributions of beam strain factors at 2% roof drift ratio due to pushover loading

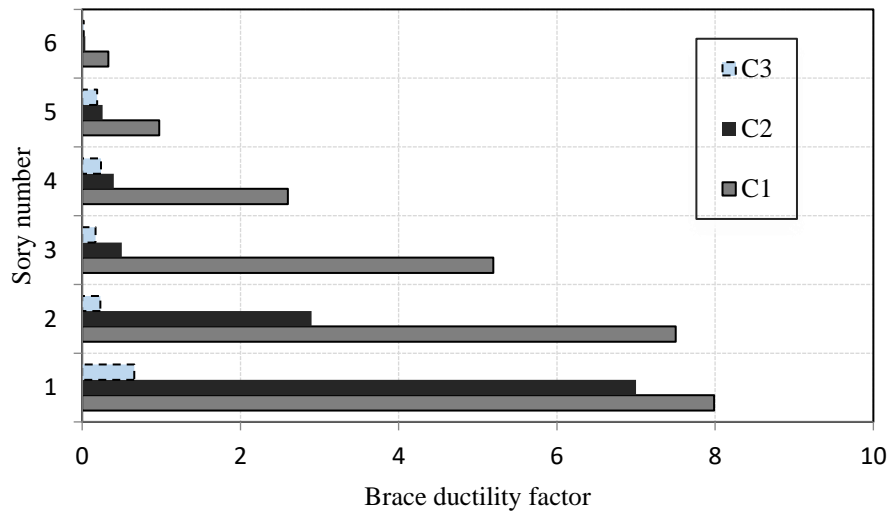


**Figure12:** The Distributions of BRB ductility factors at 2% roof drift ratio due to pushover analysis

## 5. Free vibration characteristics of the frames

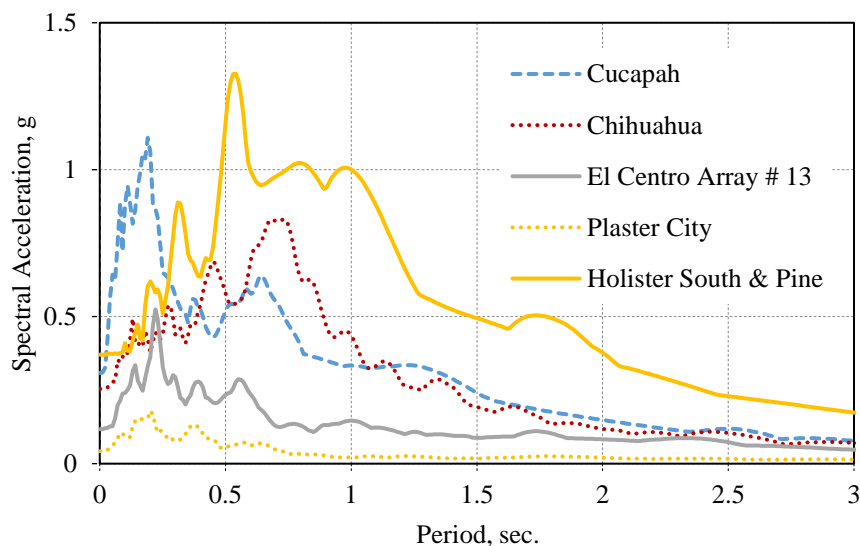
The fundamental periods of the three braced cases and the original RC frame calculated by the SeismoStruct computer program are presented in Table 7. As expected, the fundamental periods of the braced frames decrease with the increase in the amount of the braces. This behavior is attributed to the increase in the initial lateral stiffness of the braced frames with the increase in the amount of the braces.

**Table 7:** The fundamental periods of the braced cases

Design case	Period (s)	
	Mode 1 <sup>st</sup>	Mode 2 <sup>nd</sup>
Original	0.97	0.3
C <sub>1</sub>	0.86	0.283
C <sub>2</sub>	0.77	0.25
C <sub>3</sub>	0.65	0.22

## 6. Earthquake analysis

Inelastic dynamic analysis in this study is carried out using the SeismoStruct computer program. The structural masses are assumed to be lumped at the frame nodes and the effect of the geometric nonlinearity (P \_ D effect) is considered in the analysis. Gravity loads are applied on the frame during the earthquake analysis and are considered equal to the dead loads plus half of the live loads. The time-history analysis is performed using the direct integration technique considering a time step of 0.005 s and a Rayleigh damping which is defined to achieve 5.0% viscous damping in the first two natural modes of the building. Ten ground motion records that cover a wide range of frequency contents and durations are utilized in the present study. The selected earthquakes are scaled to achieve peak ground accelerations (PGAs) range from 0.1 g to 0.4 g for each record. The Earthquake data and site information are summarized in Table 8 and the response spectra of the selected records are shown in Figures. (13 and 14).

**Figure 13 :** Spectral accelerations of the selected earthquake records.

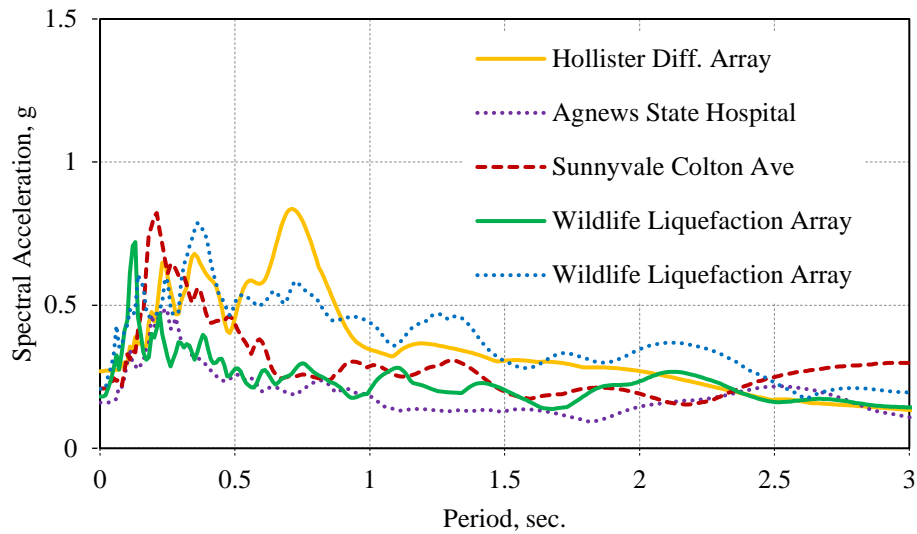


**Figure 14:** Spectral accelerations of the selected earthquake records

The seismic performances of the investigated frames are evaluated using different performance parameters which include the roof drift ratio, the maximum story drift ratio, the brace ductility demands and the maximum strain responses of the frame members. The mean plus one standard deviation ( $M+SD$ ) values of the performance parameters are used as the basis for the seismic performance evaluations. Figure (15) shows the relationships between the PGA and ( $M+SD$ ) of the roof drift ratio of the original frame and the braced cases. The results shown in Figure (15) show a significant reduction in the roof drift response with the increase in the amount of the braces. At the design PGA level (0.15 g), the roof drift ratios reached 2.5%, 1.63%, 1.26% and 1.08% for the original RC frame and the three braced cases  $C_1$ ,  $C_2$  and  $C_3$ , respectively.

Figure (16) shows the relationships between the PGA and ( $M+SD$ ) of the maximum story drift ratios of the original frame and the braced cases. The results shown in Figure (16) exhibit significant decrease in the maximum story drift response with the increase in the amount of braces. For the original RC frame and the three braced cases  $C_1$ ,  $C_2$  and  $C_3$ , respectively, the maximum story drift ratios reached 1%, 0.71%, 0.55%, 0.44% at 0.15g and 3.4%, 2.38%, 1.91%, 1.26% at 0.4g.

The distributions of the ( $M+SD$ ) story drift ratios along the frame height at 0.15 g and 0.4 g are shown in Figure 17 (a) and (b), respectively. The results shown in Figure (17) a and b indicate significant improvement in the distribution of story drifts with the increase in the amount of braces.

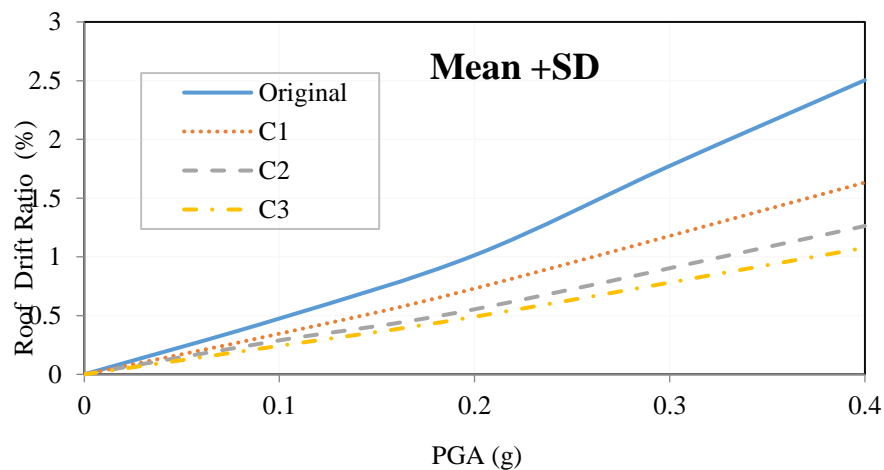
Figure (18) shows the relationships between the ( $M+SD$ ) maximum column strain factors and the PGA of the earth-quakes. The results presented in Figure (18) indicate that the maximum column strain factor increases with the increase in the amount of steel braces. This behavior can be attributed to the axial force increase in the frame columns due to the existing of the BRBs. For the original RC frame and the three braced cases  $C_1$ ,  $C_2$  and  $C_3$ , respectively, the ( $M+SD$ ) maximum

column strain factors reached 0.81, 0.68, 0.71, 0.8 at 0.15g and 3.2, 2.2, 2.6, 4.25 at 0.4g. The distribution of column strain factors along the frame stories corresponding to 0.15 g and 0.4 g is shown in Figure 19(a) and (b), respectively. The maximum column strain factors occurred in the first-story for all the design cases.

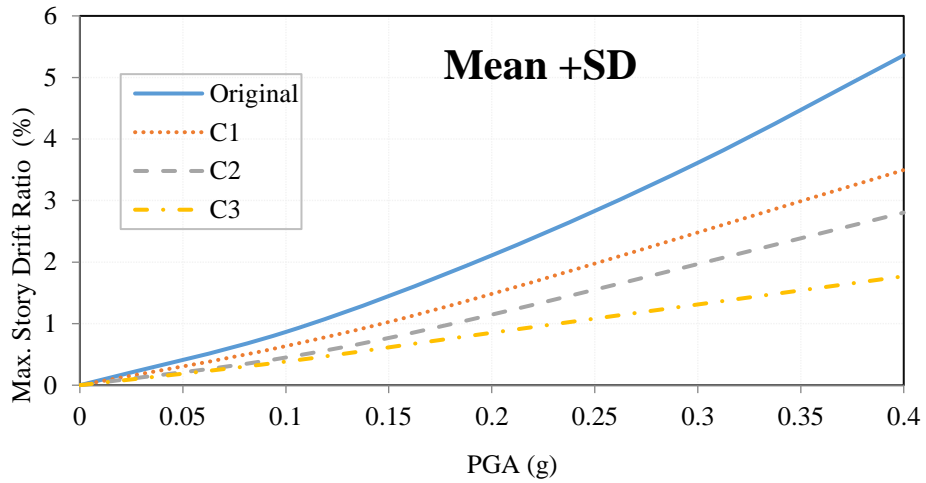
Figure (20) shows the relationships between the (M +SD) maximum beam strain factors and the PGA of the earthquakes. The results presented in Fig. 20 indicate that the maximum beam strain factor decreases with the increase in the amount of steel braces. This behavior can be attributed to the reduction in story drifts due to the existing of the BRBs. For the original RC frame and the three braced cases S1, S2 and S3, respectively, the (M + SD) maximum beam strain factors 5.4, 3.7, 2.3, 1.94 at 0.15g and 19.6, 13.8, 11.4, 8.07 at 0.4g. The distribution of beam strain factors along the frame stories corresponding to 0.15 g and 0.4 g is shown in Figure 21(a) and (b), respectively.

Figure (22) shows the relationships between the (M+SD) BRB ductility demands and the PGA of the earthquakes. The results presented in Figure (22) indicate that the maximum BRB ductility demands decreases with the increase in the amount of steel braces. This behaviour can be attributed to the reduction in story drifts due to the existing of the BRBs. For the three braced cases C<sub>1</sub>, C<sub>2</sub> and C<sub>3</sub>, respectively, the (M+SD) BRB ductility demands reached 2.11, 1.32 and 0.37 at 0.15g and 6.8, 5.4 and 0.9 at 0.4g.

The distribution of BRB ductility demands along the frame stories corresponding to 0.15g and 0.4g are shown in Fig.23 a and b, respectively. The maximum BRB ductility demands occurred in the first-story for all the design cases. The results shown in Figure 23 (a) and (b) also show a significant reduction in the maximum BRB ductility demands with the increase in the amount of braces which is attributed to the reduction in story drift demands with the increase in the amount of braces.



**Figure 15:** Relationships between the PGA and the (M +SD) roof drift ratios



**Figure 16:** Relationships between the PGA and the (M +SD) maximum story drift ratios.

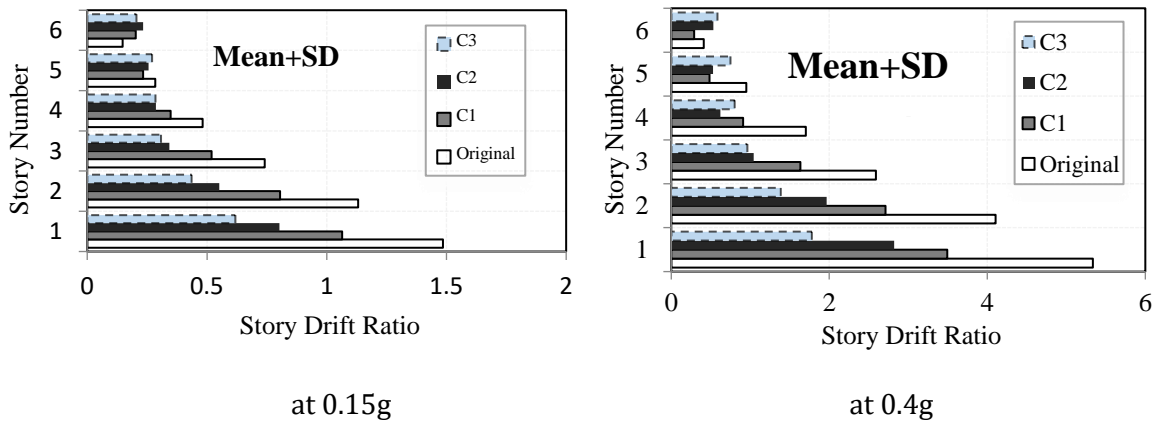


**Figure 17:** The distributions of the (M + SD) story drift ratios along the frame height.

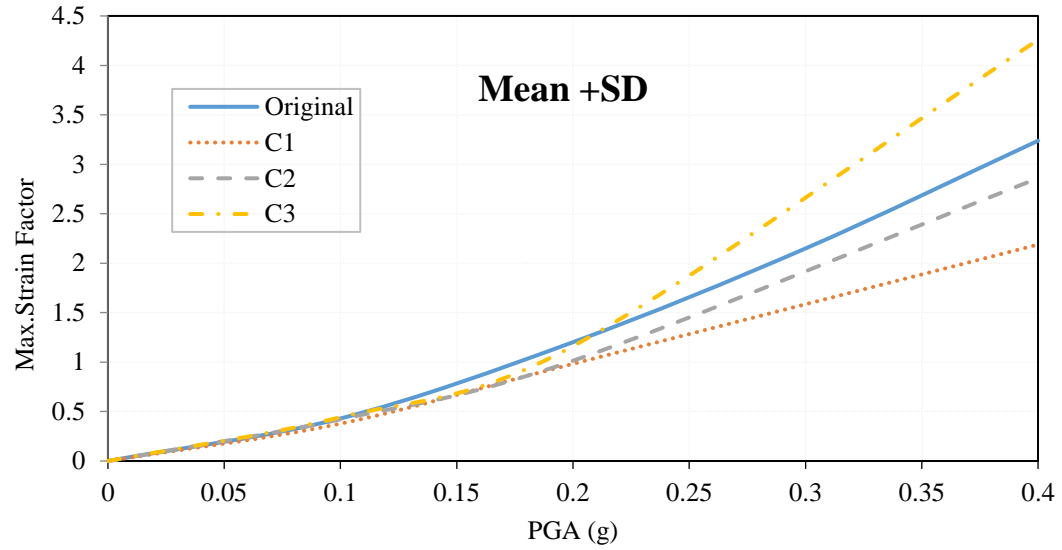


Figure 18: Relationships between the PGA and the (M + SD) maximum column strain factors.

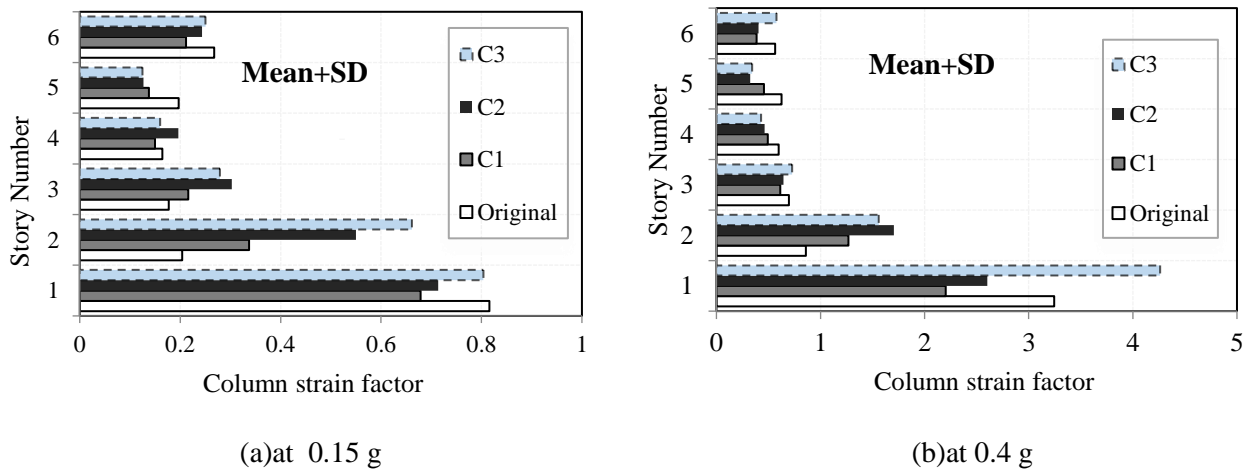


Figure 19: The distributions of the (M + SD) column strain factors along the frame height.

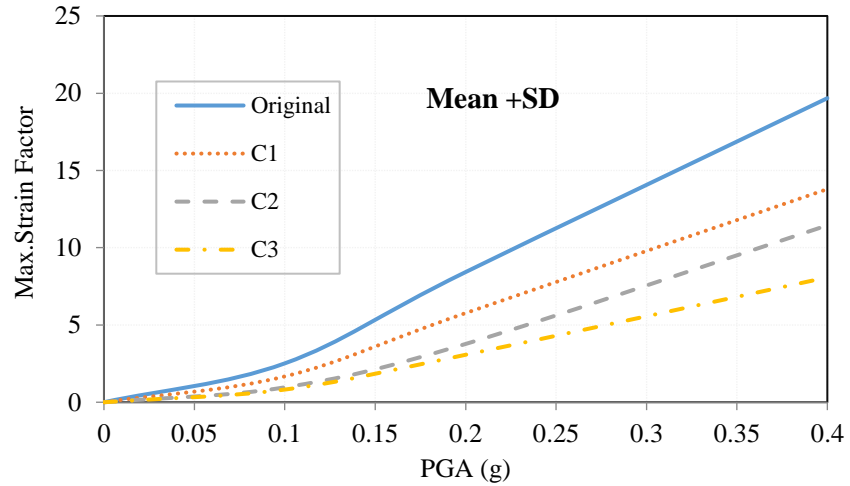


Figure 20: Relationships between the PGA and the (M + SD) maximum beam strain factors

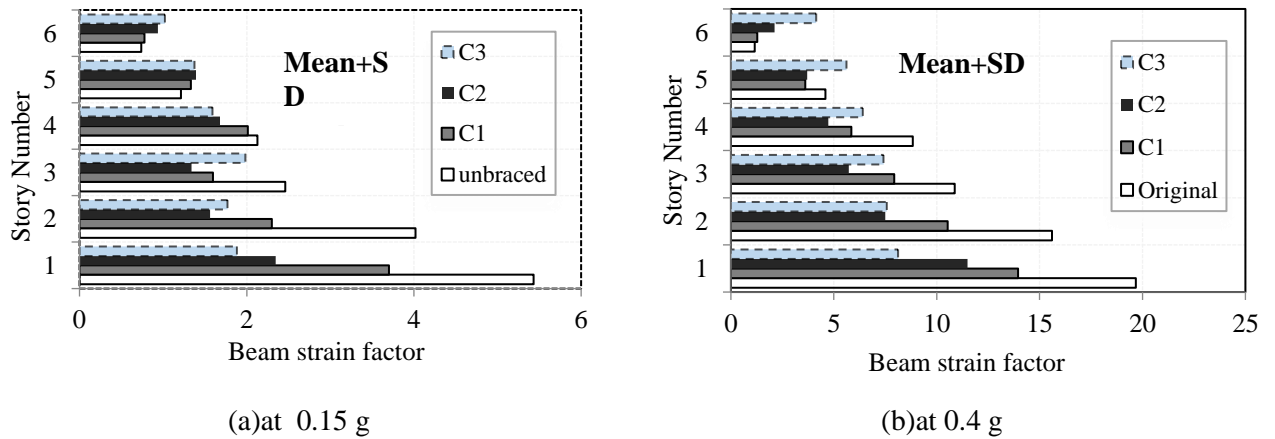
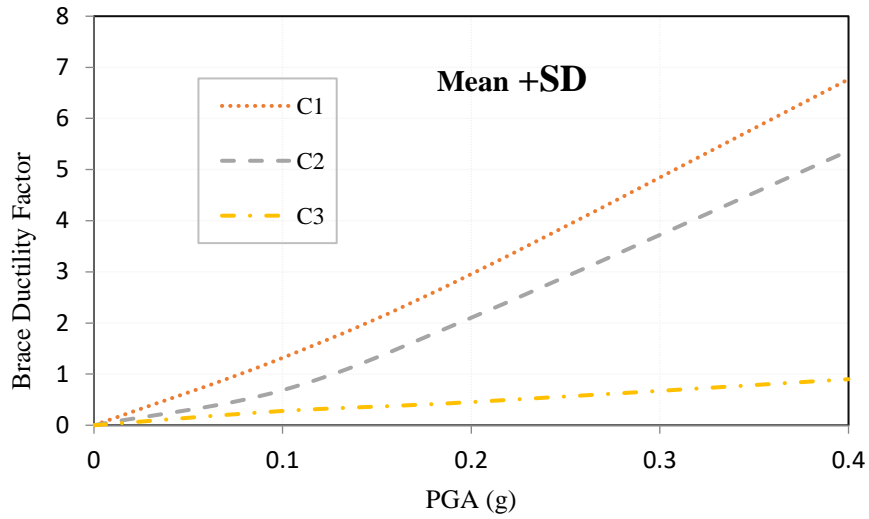
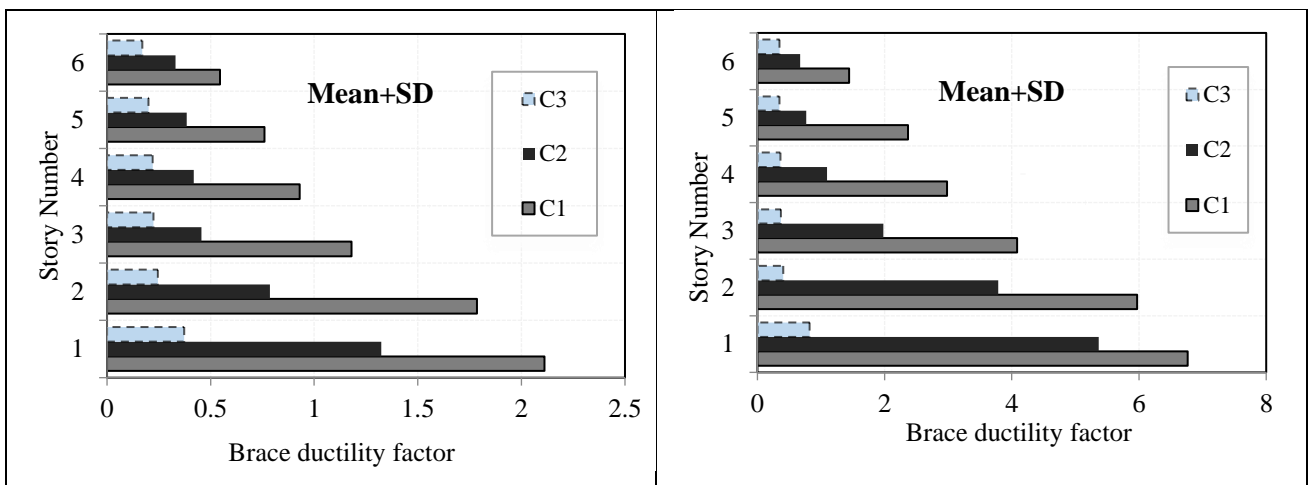


Figure 21: The distributions of the (M + SD) beam strain factors along the frame height.



**Figure 22:** Relationships between the PGA and the (M+SD) BRB ductility factors



(a) at 0.15 g

(b) at 0.4 g

**Figure 23:** The distributions of the (M + SD) BRB ductility factors along the frame height.

## 7.The PGA capacities of the frames

---

The performance limits defined by the FEMA-356 (2000) and Fahnestock et al. (2003) are used for calculating the corresponding PGA capacities of the design cases using the data presented previously in this chapter. The calculated PGA capacities of the original RC frame and the three braced cases  $C_1$ ,  $C_2$  and  $C_3$  are found equal to 0.19g, 0.268g, 0.325g, and 0.435g, respectively. This indicates that the PGA capacities of the braced frames  $C_1$ ,  $C_2$  and  $C_3$  are 41%, 71.1% and 129%, respectively, higher than the PGA capacity of the original RC frame.

## 8.Conclusions

---

The seismic upgrading of a 6-story RC-building using chevron BRBs has been evaluated by static pushover analysis and time history earthquake analysis. Based on the results obtained the following conclusions are drawn.

- 1- The use of BRBs in bay in each of the perimeter frames of the RC building results in a significant improvement to the base shear capacity of the RC building. In the current study, an increase in the base shear capacity up to 150% from the base shear capacity of the original RC building has been achieved by the BRBs.
- 2- Strengthening of RC buildings with BRBs is an efficient technique in increasing the PGA capacity of the RC buildings. The results of this study indicate the increase in the PGA capacity of the RC frames with the increase in the amount of the braces. And The PGA capacities of the braced frames  $C_1$ ,  $C_2$  and  $C_3$  are 41%, 71.1% and 129%, respectively, higher than the PGA capacity of the original RC frame.
- 3- Bracing of the perimeter frames imposes significant axial force demands on the columns and the foundations of the braced bay which requires cross section enlargement of the columns and strengthening of the foundations.

## References:

1. A.C. Masri, S.C. Goel, Seismic design and testing of an RC slab -column frame strengthened by steel bracing, *Earthquake Spectra* 12 (4) (1996) 645–666.
2. T.D. Bush, E.A. Jones, J.O. Jirsa, Behavior of RC frame strengthened using structural-steel bracing, *ASCE J. Struct. Eng.* 117 (4) (1991) 1115–1126.
3. M.R. Maheri, A. Sahebi, Use of steel bracing in reinforced concrete frames, *Eng. Struct.* 19 (12) (1997) 1018–1024.
4. F. Liu, L. Wang, X. Lu, Experimental investigations of seismic performance of unretrofitted and retrofitted RC frames, in: 15<sup>th</sup> World Conference of Earthquake Engineering 2012, Lisbon, Portugal.
5. Y. Alashkar, Comparative study of seismic strengthening of RC buildings by steel bracings and concrete shear walls, *Int. J. Civil Struct. Eng. Res.* 2 (2) (2014) 24–34.
6. A. Farghaly, A.M. Abdallah, Evaluation of seismic strengthening techniques used in old reinforced concrete buildings, *IOSR J. Eng.* 04 (06) (2014) 14–22.
7. Y.E. Ibrahim, Assessment of seismic retrofitting techniques of RC structures using fragility curves, *Int. J. Civil Struct. Eng. Res.* 5 (3) (2016) 24–34.
8. Hosseini, S. Abu Bakar, S. Bagherinejad, K. Hosseinpour, E. PUSHOVER ANALYSIS OF REINFORCED CONCRETE BUILDING WITH VERTICAL SHEAR LINK STEEL BRACES. *Malaysian Journal of Civil Engineering* 27(2):169-179 (2015).
9. R. Sabelli, W.A. Lopez, Design of buckling-restrained braced frames, in: North America Steel Construction Conference, 2014.
10. J. Newell, C. Uang, G. Benzoni, Subassembly Testing of Core Brace Buckling Restrained Braces (G Series) Report No. TR-06/ 01, Department of Structural Engineering, University of California, San Diego, California, 2006.
11. P. Clark, I. Aiken, K. Kasai, E. Ko, I. Kimura, Design Procedures for Buildings Incorporating Hysteretic Damping Devices, 69th Annual Convention, Structural Engineers Association of California, SEAOC, Sacramento, 1999.
12. Fahnestock LA, Sause R, Ricles JM. Analytical and experimental studies on buckling restrained braced composite frames. International Workshop on Steel and Concrete Composite Construction 2003, Taipei, Taiwan.
13. Sarno, L.D., Elnashai, A.S. (2008) "Bracing Systems for Seismic Retrofitting of Steel Frames", *Journal of Constructional Steel Research*: 65 (2009), 452-465.
14. Deulkar, W., Modhera, C., & Patil, H. (2010). Buckling Restrained Braces for Vibration Control of Building Structures. *IJRRAS* 4, 363-372.
15. O. Atlayan, F. Charney, Hybrid buckling-restrained braced frames, *J. Constr. Steel Res.* 96 (2014) 95–105.
16. D.J. Miller, Development and Experimental Validation of Self-Centering Buckling-Restrained Braces with Shape Memory Alloy, University of Illinois at Urbana-Champaign, 2011 (M.Sc Thesis).
17. ECP-201: Egyptian Code for Calculating Loads and Forces in Structural Work and Masonry, Housing and Building National Research Center, Ministry of Housing, Utilities and Urban Planning, Cairo, 2012.
18. ECP-203: Egyptian Code of Practice for Design and Construction of Concrete Structures, Research Center for Housing and Construction, Ministry of Housing, Utilities and Urban Planning, Cairo, 2007.
19. SeismoStruct v7.0– A computer program for static and dynamic nonlinear analysis of framed structures, available from <http://www.seissoft.com>, 2014.
20. Mander JB, Priestley MJN, Park R. Theoretical stress-strain model for confined concrete. *Journal of Structural Engineering* 1988; 114(8): 1804-1826.
21. Martinez-Rueda JE, Elnashai AS. Confined concrete model under cyclic load. *Materials and Structures* 1997; 30(197); 139-147.